Elimination of Multiple Estimation for Fault Location in Radial Power Systems by Using Fundamental Single-End Measurements

G. Morales-España, J. Mora-Flórez, *Member, IEEE*, and H. Vargas-Torres

***Abstract*—This paper presents a conceptual approach for eliminating the multiple estimation problem of impedance-based fault location methods applied to power distribution systems, using the available measurements of current and voltage fundamentals at the power substation. Three test systems are used to identify the faulted lateral obtaining high performance, even in the case of similar feeder configurations. This approach shows that it is possible to obtain a unique fault location, eliminating the problem of multiple estimation in tree-shaped radial systems using the single-end measurements at the distribution substation. Finally, this approach also contributes to improve the power continuity indexes in distribution systems by the opportune zone fault location.**

***Index Terms*—Fault location, multiple estimation, radial power systems, service continuity indexes.**

I. Introduction

SERVICE continuity in power transmission and distribution systems is nowadays considered as an important issue, mainly because of the deregulation of the current open markets. The most common measure of service continuity are indexes such as the system average interruption frequency index (SAIFI) and system average interruption duration index (SAIDI) [1], [2].

Faults cause supply interruptions that are responsible of poor service continuity indexes. It is widely accepted using fault locators to reduce the impact of such faults on the SAIFI and SAIDI indexes in three ways: first, fault location helps to speed up the restoration process; second, by locating the faulted node it is possible to perform sectionalizer switching operations to reduce the affected area; and finally, by locating nonpermanent faults it is possible to perform scheduled preventive maintenance tasks to avoid future faults.

Some efficient approaches have been proposed for fault location in power transmission systems [3]. However, these algorithms are not useful for fault location in radial systems, specifically in distribution systems due to some distinctive characteristics as: a) voltage and current are available typically only at the distribution substation; b) presence of single- and double-phase laterals; c) tapped loads along the lines and their unknown hourly variation; d) single- or three-phase lateralsl; and e) the nonuniform development of the network and loads is responsible of lines with heterogeneous sections (presence of different conductor gauges, combination of overhead lines and underground cables, among others). In addition, variations in the short circuit level caused by changes in the system topology and the equivalent generation source imply the variation of the measurements for each specific fault condition.

Several methods have been proposed for fault location in power distribution systems. Most of them estimate the equivalent distance to the fault based on the impedance estimation as seen from the substation. The pre-fault and fault effective values (rms) of the fundamental currents and voltages at the substation are used for this purpose [4]–[6]. Then, the faulted section is estimated following an iterative procedure where the impedance obtained from the line model, considering a possible fault in each system node, is compared with the equivalent impedance estimated from measurements. The fault point in the section line could be estimated according to the reactance analysis as it is described in [5], [6]. There are several methods that follow this basic principle for fault location in power distribution systems [7].

The common drawback of the impedance-based methods is the multiple-estimation problem given by the existence of multiple points (usually far away one from each other) in the power distribution systems that fulfill the equivalent impedance condition. Consequently, these methods provide precise (accurate distance to the fault) but uncertain fault locations (multiple section lines are at the same electrical distance). This is the main disadvantage when applying these methods in real power systems, since the existence of multiple possible fault locations in a large geographical area does not solve the real need of a fast fault location.

One of the most common proposed solutions for multiple estimation of fault location is using fault sensor devices which detect and distinguish abnormal current and voltage events at the overhead power lines [3]. This is not an economic alternative due to the high number of feeders, the cost of devices, and the crew needed in maintenance tasks related to such sensor devices.

On the other hand, many researchers have recently addressed this problem by using knowledge-based techniques to assist fault location, exploiting the existence of previous experiences and contextual information [2], [8]–[11]. The main drawbacks of these methods are the use of a large and usually not available

Manuscript received March 12, 2008; revised June 17, 2008. Current version published June 24, 2009. Paper no. TPWRD-00202-2008.

G. Morales-España is with the Delft University of Technology, Delft, The Netherlands (e-mail: G.A.MoralesEspana@student.tudelft.nl; g.morales.espana@gmail.com).

J. Mora-Flórez is with the Universidad Tecnológica de Pereira, Pereira, Colombia (e-mail: jjmora@utp.edu.co).

H. Vargas-Torres is with the Universidad Industrial de Santander, Bucaramanga, Colombia (e-mail: hrvargas@uis.edu.co).

Digital Object Identifier 10.1109/TPWRD.2009.2013400

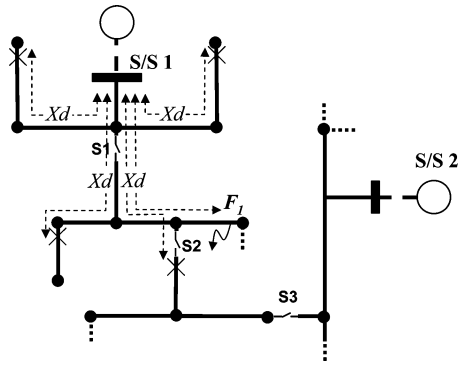

Fig. 1. Example of the multiple estimation problem of the impedance-based fault location methods, in the case of fault F1.

amount of information associated to fault registers, and the inherent lack of confidence of these black box methodologies due to the difficulties to determine the nature of the obtained solution. Moreover, an additional problem is related to the economic and computational cost of such approaches, which makes these prohibitive for distribution utilities, considering the high number of power substations.

In this paper, a novel concept applicable to fault distance estimation methods which only uses single-end measurements of the current and voltage fundamentals at the distribution substation is presented. The performance of the proposed concept is shown on a simple application where the classical reactance-based fault location method is selected. Therefore, this paper shows that it is possible to obtain a unique fault location, eliminating the problem of multiple estimation in three-phase and tree-shaped radial power systems.

The paper is presented in four sections. In Section II, the methodological approach is presented. Next, in Section III the tests and the result analysis are given. Finally, Section IV is aimed to conclude and summarize the main contributions of this research.

II. Methodological Approach

A. Multiple Estimation of the Faulted Node

The problem of the multiple estimation of the faulted node is presented by considering the power distribution system proposed as example in Fig. 1. This is a typical distribution system where two normally closed sectionalizers (S1 and S2) are used to supply the system from the power substation S/S1. There is a supplementary normally open sectionalizer (S3) used to give an additional power source (S/S2) in the case of faults, as a low cost strategy for improving the service continuity in the distribution system.

In the proposed example and by using an impedance-based method to locate the fault F1, there is a decision problem because it is possible to obtain five different locations at the same electrical reactance Xd, as it is presented in Fig. 1.

By identifying only one faulted node, the multiple estimation problem is avoided, and it is possible to give accurate information to the maintenance crew in order to quickly find and restore the fault. Additionally, by identifying the faulted node, it is possible to perform switching actions (opening S1–S2 and closing S3) to immediately restore the service in un-faulted lines, although the fault remains unattended. By the simple switching actions index SAIDI is improved by the immediately restoration of load located between S3 and S2, reducing the nonsupplied load.

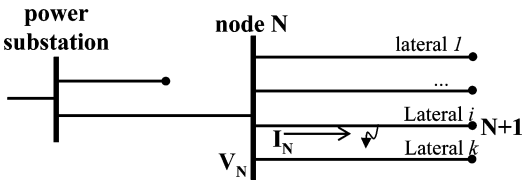

Fig. 2. Tree-shaped power distribution system.

B. Proposed Fault Location Method

The reactance-based fault location method proposed in [5], [6] is used to show, in a simple manner, the application of the proposed concept. Better results could be obtained if more elaborated methods as these proposed in [4], [12]–[15], among others, are used. The main problem of the proposed concept applied in more elaborated fault location methods is related to the deduction of the equation sets.

Considering a fault in lateral i ($i = 1, 2, 3, \ldots, k$; where k is the total number of laterals), as presented in Fig. 2, voltage and current are obtained by using the voltage and currents measured at the power substation and applying a simple load flow upstream the supposed faulted lateral $(\text{lateral } i)$. To perform this procedure it is necessary to know the load distribution as is proposed in [16]–[18].

Taking into account the unbalanced nature of the power distribution systems, the proposal here presented considers phase analysis instead of symmetrical components. The line impedance in lateral i between nodes N and $\mathrm{N}+1(\mathbf{Z_{line}})$, and the accumulated load impedance from $\mathrm{N}+1$ to the lateral end $(\mathbf{Z_{Load}})$ are given by (1) and (2), respectively

$$\mathbf{Z_{line}} = \begin{bmatrix} Z_{aa} & Z_{ab} & Z_{ac} \\ Z_{ba} & Z_{bb} & Z_{bc} \\ Z_{ca} & Z_{cb} & Z_{cc} \end{bmatrix} \tag{1}$$

$$\mathbf{Z_{Load}} = \begin{bmatrix} Z_{La} & Z_{Lab} & Z_{Lac} \\ Z_{Lba} & Z_{Lb} & Z_{Lbc} \\ Z_{Lca} & Z_{Lcb} & Z_{Lc} \end{bmatrix}. \tag{2}$$

The classical reactance-based fault location method only takes into account the faulted phases and neglects the load effect. In the proposed approach, all three phases and the loads at the nonfaulted phases are considered. The proposed fault location method also considers the fault type as it is following presented, for the four fault types.

1) Single-Phase Faults: Considering the power system in Fig. 3, (3) and (4) are obtained

$$\mathbf{V_N} = \mathbf{Z_{eq}}\mathbf{I_N}$$
$$\begin{bmatrix} V_a \\ V_b \\ V_c \end{bmatrix} = \mathbf{Z_{eq}} \begin{bmatrix} I_a \\ I_b \\ I_c \end{bmatrix} \tag{3}$$

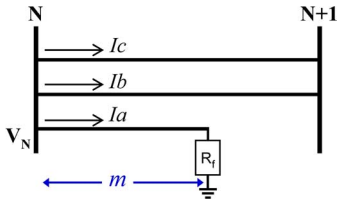

Fig. 3. Equivalent three-phase circuit for lateral i in the case of single-phase fault.

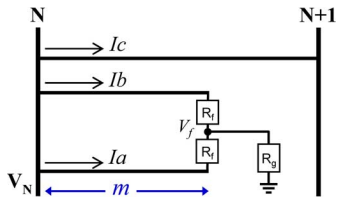

Fig. 4. Equivalent three-phase circuit for *lateral* i in the case of double-phase to ground fault.

$$\mathbf{Z_{eq}} = \begin{bmatrix} mZ_{aa} + R_f & mZ_{ab} & mZ_{ac} \\ mZ_{ba} & Z_{bb} + Z_{Lb} & Z_{bc} + Z_{Lbc} \\ mZ_{ca} & Z_{cb} + Z_{Lcb} & Z_{cc} + Z_{Lc} \end{bmatrix}. \quad (4)$$

In (4), load is considered in the nonfaulted phases to give a better approach than the used in the classical reactance-based fault location method. From the first row of (3), the fault distance m is obtained as presented in (5) as

$$m = \frac{\text{imag}\left(\frac{V_a}{I_a}\right)}{\text{imag}\left(Z_{aa} + Z_{ab}\frac{I_b}{I_a} + Z_{ac}\frac{I_c}{I_a}\right)}. \quad (5)$$

In addition, another two linear independent equations are obtained from the complex equation set presented in (3). The two additional possible solutions of m, only take into account the imaginary components, because this part remains relatively constant with variations of R_f. These equations are presented in (6) and (7) as

$$m_1 = \frac{\text{imag}\left(\frac{V_a - V_b + V_c}{I_a} + B\frac{I_b}{I_a} + C\frac{I_c}{I_a}\right)}{\text{imag}\left(Z_{aa} - Z_{ba} + Z_{ca} + A\right)} \quad (6)$$

$$m_2 = \frac{\text{imag}\left(\frac{V_a + V_b - V_c}{I_a} - B\frac{I_b}{I_a} - C\frac{I_c}{I_a}\right)}{\text{imag}\left(Z_{aa} + Z_{ba} - Z_{ca} + A\right)} \quad (7)$$

where constants A, B, and C are given in (8) as

$$\begin{aligned} A &= Z_{ab}\frac{I_b}{I_a} + Z_{ac}\frac{I_c}{I_a} \\ B &= Z_{bb} + Z_{Lb} - Z_{cb} - Z_{Lcb} \\ C &= Z_{bc} + Z_{Lbc} - Z_{cc} - Z_{Lc}. \end{aligned} \quad (8)$$

According to the previously presented information, the most suitable equation to estimate the fault distance is the presented in (5), where the load current is neglected at the faulted phase due to its low effect in the total fault current measured at the power substation. The load current is really significant at the nonfaulted phases, causing a voltage drop due to the mutual impedance. Additionally and starting from (5), the alternative option to estimate the fault distance m is by using information contained in the nonfaulted phases as it is presented in (6) and (7).

By using (5), the presented approach is similar to the one proposed in the reactance-based fault location method. Equations (6) and (7) are approximations of the distance obtained in (5), but considering the behavior of the entire lateral (loads at the nonfaulted phases and three-phase measurements of voltage and current).

Using the proposed equations it is possible to determine the faulted lateral, because the behavior of the three-phase measurements is unique for each lateral, in the case of existing differences in load or line impedance parameters. Then, in the case of single-phase faults it is possible to obtain one fault distance by using the faulted phase measurements as it is presented in (5). Next, by using three-phase measurements it is possible to compute two additional possible distances by using (6) and (7) to obtain an error as it is presented in (9) as

$$\text{Error}_i = \frac{1}{n}\frac{\sum_{j=1}^{n}|m - m_j|}{|m|} \quad (9)$$

where n is the number of possible additional distances (in case of single-phase faults, this number is two).

The error computed using (9) gives the information related to the differences in the distance obtained using only the information of the faulted phase and the computed using the three-phase measurements. Then, the faulted lateral is obtained determining the lowest error. In the case of computing the same error at the nonfaulted laterals, this is bigger than the previous case, because the measurements at the nonfaulted phases reflect the behavior of the faulted lateral.

In the case of double- and three-phase faults, the analysis is similar to the one presented for single-phase faults.

2) Double-Phase to Ground Faults: From Fig. 4, (10) and (11) are obtained in the case of phase-to-phase faults

$$\begin{bmatrix} V_a - V_f \\ V_b - V_f \\ V_c \end{bmatrix} = \mathbf{Z_{eq}} \begin{bmatrix} I_a \\ I_b \\ I_c \end{bmatrix} \quad (10)$$

$$\mathbf{Z_{eq}} = \begin{bmatrix} mZ_{aa} + R_f & mZ_{ab} & mZ_{ac} \\ mZ_{ba} & mZ_{bb} + R_f & mZ_{bc} \\ mZ_{ca} & mZ_{cb} & Z_{cc} + Z_{Lc} \end{bmatrix}. \quad (11)$$

From the first two rows of (10), the fault distance m is obtained as it is presented in (12) as

$$m = \frac{\text{imag}\left(\frac{V_a - V_b}{I_a - I_b}\right)}{\text{imag}\left(\frac{D \cdot I_a + E \cdot I_b + F \cdot I_c}{I_a - I_b}\right)} \quad (12)$$

where constants D, E, and F are given by (13)

$$\begin{aligned} D &= Z_{aa} - Z_{ba} \\ E &= Z_{ab} - Z_{bb} \\ F &= Z_{ac} - Z_{bc}. \end{aligned} \quad (13)$$

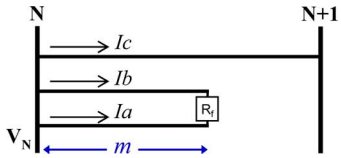

Fig. 5. Equivalent three-phase circuit for *lateral* i in the case of phase-to-phase fault.

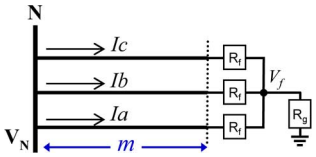

Fig. 6. Equivalent three-phase circuit for *lateral* i in the case of three-phase fault.

From (10), it is possible to obtain another linear independent equation as it is presented in (14)

$$m_1 = \frac{\text{imag}\left(\frac{V_a - V_b - V_c}{I_a - I_b} + (Z_{cc} + Z_{Lc})\frac{I_c}{I_a - I_b}\right)}{\text{imag}\left(\frac{(D - Z_{ca})I_a + (E - Z_{cb})I_b + F \cdot I_c}{I_a - I_b}\right)}. \quad (14)$$

The distance obtained from (14) is compared to the one obtained in (12) by using (9). In this case, $n = 1$. Similar to the single-phase fault case, the faulted lateral is obtained by determining the lowest error.

3) Phase-to-Phase Faults: By considering the equivalent circuit presented in Fig. 5, the equations obtained are the same as the ones presented in the case of double-phase to ground faults (these are not influenced by R_g). As a result, (12) to (14) are used in case of phase-to-phase faults.

4) Three-Phase Faults: In the case of three phase faults, and considering the system in Fig. 6, (15) and (16) are obtained

$$\begin{bmatrix} V_a - V_f \\ V_b - V_f \\ V_c - V_f \end{bmatrix} = \mathbf{Z_{eq}} \begin{bmatrix} I_a \\ I_b \\ I_c \end{bmatrix} \quad (15)$$

$$\mathbf{Z_{eq}} = \begin{bmatrix} mZ_{aa} + R_f & mZ_{ab} & mZ_{ac} \\ mZ_{ba} & mZ_{bb} + R_f & mZ_{bc} \\ mZ_{ca} & mZ_{cb} & mZ_{cc} + R_f \end{bmatrix}. \quad (16)$$

Three linear independent equations for distance m are obtained using (15), as it is presented from (17) to (19).

$$m_1 = \frac{\text{imag}\left(\frac{V_a - V_b}{I_a - I_b}\right)}{\text{imag}\left(\frac{D \cdot I_a + E \cdot I_b + F \cdot I_c}{I_a - I_b}\right)} \quad (17)$$

$$m_2 = \frac{\text{imag}\left(\frac{V_b - V_c}{I_b - I_c}\right)}{\text{imag}\left(\frac{G \cdot I_a + H \cdot I_b + J \cdot I_c}{I_b - I_c}\right)} \quad (18)$$

$$m_3 = \frac{\text{imag}\left(\frac{V_c - V_a}{I_c - I_a}\right)}{\text{imag}\left(\frac{K \cdot I_a + L \cdot I_b + M \cdot I_c}{I_c - I_a}\right)} \quad (19)$$

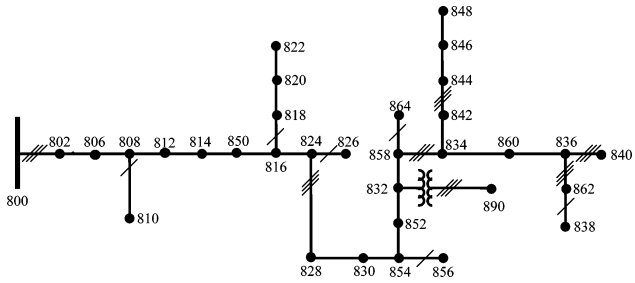

Fig. 7. IEEE 34-bus test feeder.

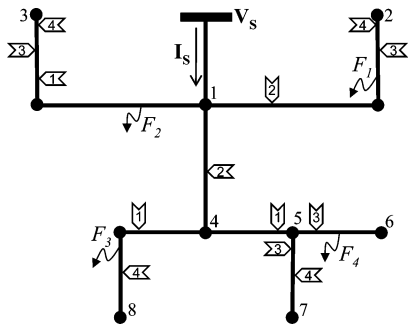

Fig. 8. Power system used to test the proposed method.

where constants G, H, J, K, L, and M are given by (20).

$$\begin{aligned} G &= Z_{ba} - Z_{ca}; \quad H = Z_{bb} - Z_{cb}; \\ J &= Z_{bc} - Z_{cc}; \quad K = Z_{ca} - Z_{aa}; \\ L &= Z_{cb} - Z_{ab}; \quad M = Z_{cc} - Z_{ac}. \end{aligned} \quad (20)$$

In this case, m is obtained as the average of those three distances, as it is proposed in (21)

$$m = \frac{1}{3}(m_1 + m_2 + m_3). \quad (21)$$

To determine the faulted feeder as previously proposed, error is computed by using (9). In this case, $n = 3$.

III. Tests and Results

A. Test System

The 24,9 kV IEEE 34-bus test feeder presented in Fig. 7 is used to test the fault location approach. The proposed system contains a three-phase main feeder, single-phase laterals, multiple conductor gauges, single- and three-phase tapped loads [19].

Additionally, two test systems were derived from the IEEE feeder. The first is presented in Fig. 8 and used in the preliminary tests. The second is presented in Fig. 2 and used for testing the case to consider the elimination of the multiple estimation in a system with similar laterals.

B. Preliminary Tests

In Fig. 8, a power distribution system composed of five laterals is proposed to perform the preliminary tests. In the case of a fault, five different locations are possible according to the information provided by the impedance-based fault location

TABLE I
FAULT LOCATION RESULTS IN PRELIMINARY

Real fault location	Estimation 1		Estimation 2		Estimation 3		Estimation 4		Estimation 5	
Section (m %)	Section (m%)	Error	Section (m%)	Error	Section (m%)	Error	Section (m%)	Error	Section (m%)	Error
1-2 (75)	1-2 (75.01)	8.4E-8	1-3 (74.84)	5.6E-4	4-5 (87.03)	0.78	4-8 (41.12)	1.62	–	–
1-3 (25)	1-3 (25.02)	4.9E-7	1-2 (25.03)	2.5E-3	1-4 (52.72)	9.1E-2	–	–	–	–
4-8 (60)	4-8 (60.00)	4.4E-11	1-3 (87.44)	4.1E-2	1-2 (87.61)	4.1E-2	5-6 (25.50)	0.229	5-7 (25.51)	0.23
5-6 (50)	5-6 (50.00)	4.1E-11	5-7 (50.01)	2.5E-3	1-3 (95.62)	4.0E-2	4-8 (72.25)	4.1E-2	1-2 (95.78)	4.1E-2

methods. Line and load parameters are obtained from the IEEE 34 node test feeder presented in Fig. 7. Configuration 300 is used for sections 0–1, 1–4 and 4–5, with 2, 3 and 2 km length respectively. Configuration 301 is used in sections 5–6, 5–7, 4–8, 1–2 and 1–3 with 2, 2, 4 and 6 km length respectively. Loads at nodes 2, 3, 4, 6, 7 and 8 are the same as the ones from the original IEEE test feeder at nodes 844, 890, 860, 830, 840 and 830, respectively. It is important to notice that the sections 5–6 and 4–8 have the same line configuration and load.

Four zero ohm faults F_1, F_2, F_3 and F_4, located in different laterals as it is presented in Fig. 8, are simulated. The possible locations are marked by using numbered arrows in the test power system as it is presented in Fig. 8, where the number n inside the arrow is related to one of the possible locations of fault F_n. In addition, the location of the faulted lateral is presented in Table I, in decremental ordering of the error magnitude, from the most to the least plausible estimation.

Although line sections 5–6 and 4–8 have the same line impedance and loads, there are not errors in the determination of the faulted lateral. This is mainly because in steady state, voltages at nodes 4 and 5 are not the same, creating a clear difference between faulted and un-faulted laterals.

C. Test Considering Similar Laterals

In case of two identical laterals (same load and line impedances) which start from the same node, the proposed methodology is not capable of identifying the faulted lateral, fortunately this is a not common situation. However, there are two cases which could seem not easy solvable, considering laterals which start from the same system node:

1) two or more laterals which have the same line impedance but different load;
2) two or more laterals which have the same load but different line impedance.

To consider the proposed cases, test are performed in a power system similar to the one presented in Fig. 2, but considering three laterals which start from node N. The system parameters are obtained form the typical IEEE 34 node test feeder [19], then laterals 1 and 2 have the following line and load impedances: $\mathbf{Z_{line1}}$ (configuration 300, 10 km length), $\mathbf{Z_{Load1}}$ (load at node 860), $\mathbf{Z_{line2}}$ (configuration 301, 10 km length), $\mathbf{Z_{Load2}}$ (load at node 830). Lateral 3 has the same line impedance of lateral 1 $(\mathbf{Z_{line3}} = \mathbf{Z_{line1}})$, and the same load of lateral 2 $(\mathbf{Z_{Load3}} = \mathbf{Z_{Load2}})$.

Fifty fault situations (faults from 2% to the 100% of the line length) performed on each lateral are used to test the proposed approach. Considering that the main purpose is to obtain the faulted lateral and not to check the performance of the distance estimation method, tests are performed only by using fault resistance of zero ohms.

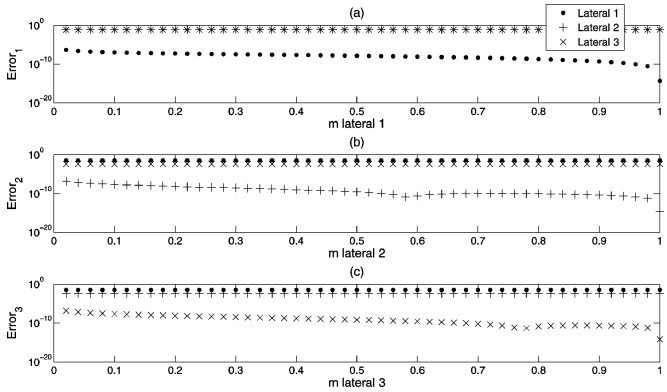

Fig. 9. Errors in fault location, considering single-phase faults at each one of the laterals 1 (a), 2 (b) y, 3 (c).

Results of the single-phase fault (a)–(g) are presented in Fig. 9. Subplots a, b, and c present the error in the cases of faults in lateral 1, 2, and 3, respectively (error is presented in logarithmic scale). Each subplot shows the error when supposing the fault in each lateral, where the dotted line $(\bullet)$ represents the error when supposing the fault at lateral 1, the crossed line $(+)$ represents the error of supposing the fault at lateral 2 and finally, the curve marked with $(\times)$ represents the error when supposing the fault at lateral 3. It is noticed from Fig. 9, how the lowest error in each subplot is always the same of the real fault location (lateral 1, 2, and 3), validating the proposed approach.

In addition, from Fig. 9 an error reduction is noticed, and it is directly related to the fault distance. This is presented because the fault location method ignores the mutual effect of the section line beyond the faulted node, and as a result, the farther the fault is, the lower the mutual effect ignored is, which also causes a decrease in the distance estimation error.

Similar behavior to the previously presented is obtained in case of phase-to-phase faults, double-phase to ground faults, and three-phase faults as presented in Figs. 10, 11, and 12, respectively.

In the case of phase-to-phase faults, as presented in Fig. 12, there are 14 wrong lateral estimations from 150 analyzed fault cases (50 in each lateral), and the difference between the error values is not as high as the obtained in case of other fault types. This is mainly because of the significant effect of the load in the behavior of voltages and currents at this fault type, even if the fault resistance is near to zero ohms. Considering that the distance method ignores the load effect, in case of fault resistances

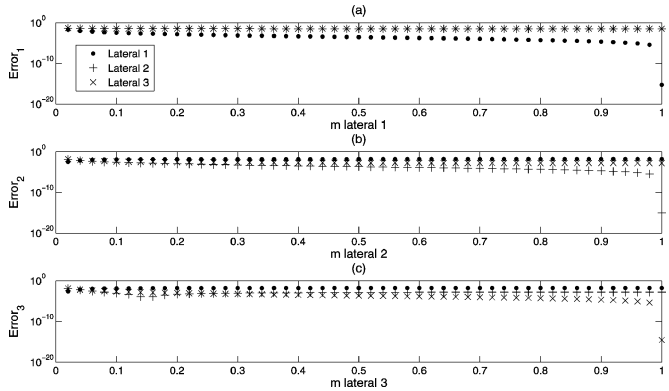

Fig. 10. Errors in fault location, considering phase-to-phase faults at each one of the laterals 1 (a), 2 (b) y, 3 (c).

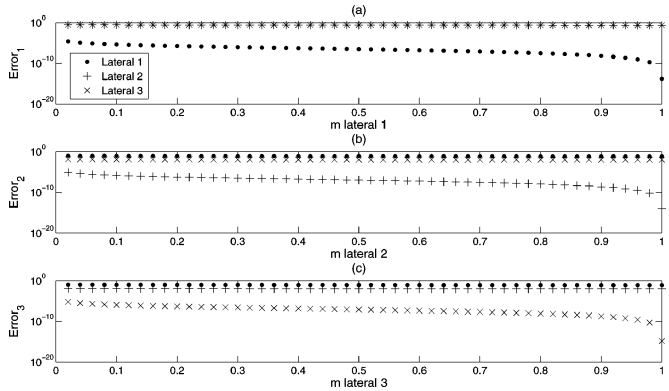

Fig. 11. Errors in fault location, considering double phase to ground faults at each one of the laterals 1 (a), 2 (b) y, 3 (c).

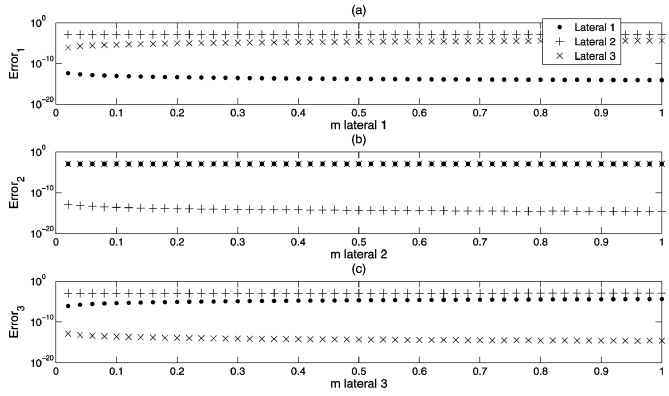

Fig. 12. Errors in fault location, considering three-phase faults at each one of the laterals 1 (a), 2 (b) y 3 (c).

different from zero, this could deteriorate the performance of the proposed approach, as it is shown in next the section.

In the case of three-phase faults as presented in Fig. 12, even having the same line impedance in laterals 1 and 3, the equivalent impedance of the nonfaulted laterals is not the same, helping to differentiate the faulted lateral.

According to the test system considered, even in the case of the same line impedance of laterals 1 and 3, and the same load at laterals 2 and 3, small differences between laterals make possible locating the faulted lateral by using measurements of voltage and current at the power substation, as it is described by the proposed methodology.

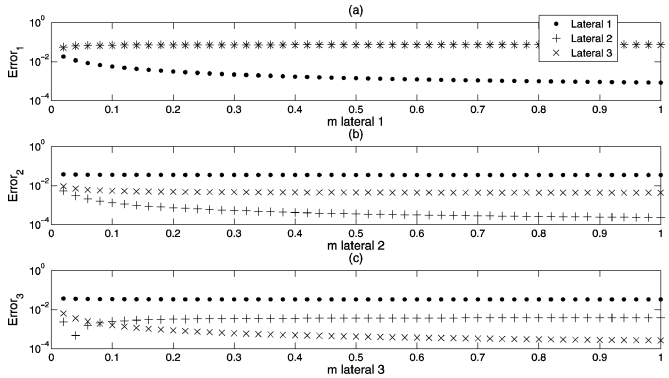

Fig. 13. Errors in fault location, considering single-phase faults with 40 Ω fault resistance at each one of the laterals 1 (a), 2 (b), y 3 (c).

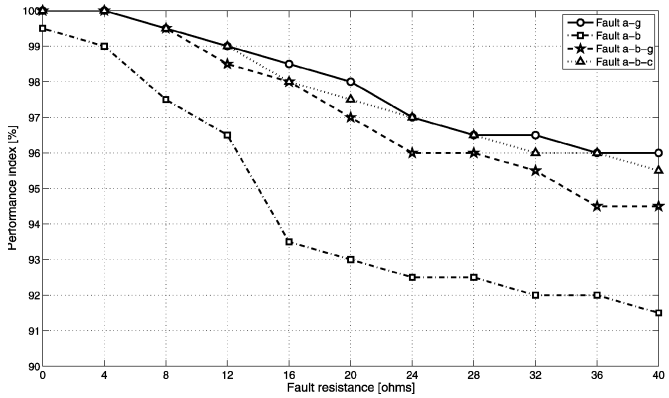

Fig. 14. Estimated performance of the proposed fault locator in the IEEE 34-bus test feeder and using a 8800 faults-database.

As complementary tests, results for the faulted lateral determination are shown in Fig. 13, in the case of a 40 Ω single-phase fault are shown. According to the figure, it is noticed how the difference among errors for each lateral is not as significant as the presented in the case of 0 Ω fault resistances plotted in Fig. 9. In addition, three wrong estimations of the faulted lateral are now obtained.

D. IEEE 34-Bus Tests

To evaluate the performance of the fault locator in the power system presented in Fig. 7, single-phase (a)–(g), phase-to-phase (a)–(b), double-phase to ground (a)–(b)–(g), and three-phase (a)–(b)–(c) faults considering 11 fault resistances from 0 Ω to 40 Ω, are used [20].

The following three-phase laterals are selected for tests: lateral from node 832 to node 890, lateral from node 832 to node 836, lateral from node 834 to node 848, lateral from node 836 to node 840 and lateral from node 836 to node 862. 1650 fault situations for each fault type were performed at the first three laterals, while only 550 faults were performed in the last two laterals. A database of 2200 faults for each type of fault, and considering four fault types, 8800 faults are then used to evaluate the performance of the proposed fault locator in the IEEE 34-bus test feeder.

The results of the estimated performance according to (22) are presented in Fig. 14. Each performance value in the figure is

TABLE II
FAULT LOCATION RESULTS IN THE IEEE 34-BUS FEEDER ($Rf = 0\ \Omega$)

Real fault location		Estimation 1		Estimation 2		Estimation 3		Estimation 4	
Section (m%)	Fault	Section (m%)	Error	Section (m%)	Error	Section (m%)	Error	Section (m%)	Error
858-834 (80)	a-g	858-834 (80)	6.26E-04	832-890 (2.59)	1.00E-01	–	–	–	–
	a-b	858-834 (80)	5.67E-03	832-890 (2.57)	7.10E-02	–	–	–	–
	a-b-g	858-834 (79.2)	7.92E-04	832-890 (2.57)	1.60E-01	–	–	–	–
	a-b-c	858-834 (80)	2.36E-15	832-890 (2.57)	6.40E-04	–	–	–	–
860-836 (50)	a-g	860-836 (50)	3.48E-04	844-846 (46.08)	2.20E-02	832-890 (3.86)	9.40E-02	–	–
	a-b	860-836 (49.5)	1.83E-03	844-846 (47.14)	1.40E-02	832-890 (3.79)	4.90E-02	–	–
	a-b-g	860-836 (50)	1.65E-04	832-890 (3.8)	1.20E-01	844-846 (47.49)	0.14	–	–
	a-b-c	860-836 (50)	3.91E-14	832-890 (3.8)	6.50E-04	844-846 (47.35)	8.80E-04	–	–
836-840 (30)	a-g	836-840 (30)	1.49E-03	836-862 (92.2)	1.30E-02	844-846 (89.09)	3.30E-02	832-890 (4.32)	8.10E-02
	a-b	836-840 (30)	1.84E-03	836-862 (92.06)	9.30E-03	844-846 (90.89)	1.90E-02	832-890 (4.22)	4.70E-02
	a-b-g	836-840 (30)	1.71E-03	836-862 (92.2)	2.80E-03	844-846 (91.27)	9.40E-02	832-890 (4.23)	0.11
	a-b-c	836-840 (30)	5.56E-14	836-862 (92.16)	5.30E-04	832-890 (4.24)	6.60E-04	844-846 (91.09)	8.20E-04
836-862 (80)	a-g	836-862 (80)	2.12E-04	836-840 (26.03)	2.40E-02	844-846 (88.17)	3.20E-02	832-890 (4.31)	8.10E-02
	a-b	836-862 (79.4)	1.09E-04	836-840 (26.07)	9.70E-03	844-846 (89.96)	2.00E-02	832-890 (4.21)	4.70E-02
	a-b-g	836-862 (80)	2.12E-04	844-846 (56.88)	1.80E-03	836-840 (26.03)	2.40E-02	832-890 (5.13)	4.70E-02
	a-b-c	836-862 (80)	2.03E-13	836-840 (26.04)	5.30E-04	832-890 (4.23)	6.60E-04	844-846 (90.16)	7.90E-04
842-844 (50)	a-g	842-844 (50)	5.19E-04	832-890 (3.18)	8.30E-02	834-860 (47.53)	0.34	–	–
	a-b	834-860 (49.18)	1.62E-03	842-844 (50)	1.10E-02	832-890 (3.14)	5.40E-02	–	–
	a-b-g	842-844 (50)	5.19E-04	832-890 (4.03)	3.90E-02	858-834 (98.8)	6.40E-02	–	–
	a-b-c	842-844 (50)	9.66E-14	834-860 (47.3)	2.90E-04	832-890 (3.15)	6.60E-04	–	–
844-846 (50)	a-g	844-846 (50)	2.54E-04	832-890 (3.91)	5.60E-02	860-836 (55.44)	1.03	–	–
	a-b	844-846 (50.12)	2.16E-03	860-836 (53.9)	1.60E-02	832-890 (3.82)	4.90E-02	–	–
	a-b-g	844-846 (50)	2.54E-04	832-890 (4.8)	2.40E-02	860-836 (97.95)	0.58	–	–
	a-b-c	844-846 (50)	3.78E-14	832-890 (3.83)	7.00E-04	860-836 (53.6)	1.10E-03	–	–

TABLE III
FAULT LOCATION RESULTS IN THE IEEE 34-BUS FEEDER ($Rf = 40\ \Omega$)

Real fault location		Estimation 1		Estimation 2		Estimation 3		Estimation 4	
Section (m%)	Fault	Section (m%)	Error	Section (m%)	Error	Section (m%)	Error	Section (m%)	Error
858-834 (80)	a-g	858-834 (82.5)	6.30E-04	832-890 (3.37)	4.50E-02	–	–	–	–
	a-b	858-834 (81.6)	5.70E-03	832-890 (2.57)	7.10E-02	–	–	–	–
	a-b-g	858-834 (76.59)	5.10E-04	832-890 (3.96)	6.50E-03	–	–	–	–
	a-b-c	858-834 (80.36)	2.40E-15	832-890 (2.57)	6.40E-04	–	–	–	–
860-836 (50)	a-g	860-836 (51.25)	3.50E-04	844-846 (37.63)	3.30E-03	832-890 (4.68)	5.40E-02	–	–
	a-b	860-836 (48.70)	1.80E-03	844-846 (46.27)	1.10E-02	832-890 (3.79)	4.90E-02	–	–
	a-b-g	860-836 (51.3)	1.70E-04	832-890 (5.24)	6.50E-03	844-846 (47.49)	0.14	–	–
	a-b-c	860-836 (50.17)	3.90E-14	832-890 (3.8)	6.50E-04	844-846 (47.35)	8.80E-04	–	–
836-840 (30)	a-g	844-846 (57.77)	3.70E-05	836-840 (31.62)	1.50E-03	836-862 (96.64)	7.10E-03	832-890 (5.14)	4.70E-02
	a-b	836-862 (63.44)	5.50E-04	836-840 (28.86)	1.80E-03	844-846 (89.94)	1.90E-02	832-890 (4.22)	4.70E-02
	a-b-g	836-840 (31.21)	1.70E-03	836-862 (92.2)	2.80E-03	832-890 (5.68)	1.10E-02	844-846 (91.27)	9.40E-02
	a-b-c	836-840 (30.26)	5.60E-14	836-862 (92.16)	5.30E-04	832-890 (4.24)	6.60E-04	844-846 (91.09)	8.20E-04
836-862 (80)	a-g	836-862 (81.36)	2.10E-04	844-846 (56.88)	1.80E-03	836-840 (26.03)	2.40E-02	832-890 (5.13)	4.70E-02
	a-b	836-862 (78.76)	1.10E-04	836-840 (33.62)	3.20E-04	844-846 (89.03)	2.00E-02	832-890 (4.21)	4.70E-02
	a-b-g	836-862 (79.87)	1.20E-05	832-890 (5.67)	1.10E-02	836-840 (26.03)	2.30E-02	844-846 (90.33)	9.40E-02
	a-b-c	836-862 (80.09)	2.00E-13	836-840 (26.04)	5.30E-04	832-890 (4.23)	6.60E-04	844-846 (90.16)	7.90E-04
842-844 (50)	a-g	842-844 (51.36)	5.20E-04	832-890 (4.03)	3.90E-02	834-860 (95.83)	0.27	–	–
	a-b	834-860 (49.64)	1.00E-03	842-844 (54.42)	1.10E-02	832-890 (3.14)	5.40E-02	–	–
	a-b-g	842-844 (50.94)	1.30E-03	858-834 (87.42)	1.80E-03	832-890 (4.64)	2.60E-02	–	–
	a-b-c	842-844 (50.48)	9.70E-14	834-860 (47.3)	2.90E-04	832-890 (3.15)	6.60E-04	–	–
844-846 (50)	a-g	844-846 (52.43)	2.50E-04	832-890 (4.8)	2.40E-02	860-836 (97.95)	0.58	–	–
	a-b	844-846 (48.34)	2.00E-03	860-836 (53.9)	1.60E-02	832-890 (3.82)	4.90E-02	–	–
	a-b-g	844-846 (51.39)	5.20E-05	832-890 (5.4)	6.80E-02	860-836 (99.76)	1.44	–	–
	a-b-c	844-846 (50.15)	3.80E-14	832-890 (3.83)	7.00E-04	860-836 (53.6)	1.10E-03	–	–

related to each fault type and fault resistance, using 200 faults located along the laterals.

Tables II and III present several of the obtained results. Highlighted rows indicate some errors in the faulted lateral identification.

Faults location of 0 Ω are presented in Table II. It is noticed how for a phase-to-phase fault (a)–(b) the lowest error determines the faulted lateral as the lateral from node 834 to node 860. However, the real fault location is in the zone from node 842 to node 844 (at the 50% of the total line length), which is determined as the second possible alternative (estimation 2). In Table III, some other problems in the lateral estimation are presented in the case of 40 Ω faults.

Additionally, it is notice that higher errors are obtained in the case of double-phase faults, where the minimum performance is obtained (91.5% for 40 Ω faults). However in the case of single-phase faults in the IEEE 34-bus feeder, which are the most common in power distribution systems, the obtained performance of the proposed fault locator is higher than 96%.

IV. Conclusion

This paper presents a conceptual approach to eliminate the multiple estimation problem of the impedance-based fault location methods. Measurements of voltage and current fundamentals at the power distribution substation are used in the proposed approach.

Tests performed by considering three different power systems and the four fault types (single fault to ground, phase-to-phase, double-phase to ground, and three-phase faults), demonstrate the capability of the proposed method to determine the faulted lateral, even in the case where there are similitudes between laterals. According to the test, the proposed approach has very high performance, in the case of the analyzed circumstances of simulated faults

$$\text{performance} = \frac{\sum \text{lateral correctly identified}}{\text{Total number of faults (200)}}. \qquad (22)$$

Finally, this approach also contributes to improve the power continuity indexes in distribution systems by the opportune zone fault location. First, fault location helps to speed up the restoration process; second, by locating the fault it is possible to perform sectionalizer switching operations to reduce the affected area; and finally, by locating nonpermanent faults it is possible to perform scheduled preventive maintenance tasks to avoid future faults.

References

[1] T. A. Short, *Electric Power Distribution Handbook*, 1st ed. London, U.K.: Taylor & Francis, Apr. 2007.

[2] J. Mora-Florez, "Localización de Faltas en Sistemas de Distribución de Energía Eléctrica Usando métodos Basados en el Modelo y Métodos Basados en el Conocimiento" Ph.D. dissertation, Univ. Girona, Girona, España, 2006 [Online]. Available: http-://www.tesisenred.net/TESIS_UdG/AVAILABLE/TDX-0220107-131316//tjjmf.pdf

[3] *IEEE Guide for Determining Fault Location on AC Transmission and Distribution Lines*, IEEE Std. 37.114-2004, 2005.

[4] R. Das, "Determining the Locations of Faults in Distribution Systems," Ph.D. dissertation, Univ. Saskatchewan, Saskatoon, Canada, 1998.

[5] M. Sachdev, R. Das, and T. Sidhu, "Distribution line shunt fault locations from digital relay measurements," *Can. J. Elect. Comput. Eng.*, vol. 24, no. 1, pp. 41–47, Jan. 1999.

[6] R. Das, M. Sachdev, and T. Sidhu, "A fault locator for radial subtransmission and distribution lines," in *Proc. Power Engineering Society Summer Meeting*, 2000, vol. 1, pp. 443–448.

[7] J. Mora-Florez, J. Melendez, and G. Carrillo-Caicedo, "Comparison of impedance based fault location methods for power distribution systems," *Elect. Power Syst. Res.*, vol. 78, no. 4, pp. 657–666, Apr. 2008.

[8] G. Morales-España and A. GómezRuiz, Estudio e implementación de una herramienta basada en Máquinas de Soporte Vectorial aplicada a la localización de fallas en sistemas de distribución. Bucaramanga, Colombia, Tesis de grado, Universidad Industrial de Santander, 2005 [Online]. Available: http://tangara.uis.edu.co/biblioweb/pags/cat/popup/derautor.jsp?parametros=118738

[9] J. Mora-Florez, V. Barrera-Nuez, and G. Carrillo-Caicedo, "Fault location in power distribution systems using a learning algorithm for multivariable data analysis," *IEEE Trans. Power Del.*, vol. 22, no. 3, pp. 1715–1721, Jul. 2007.

[10] G. Morales-España, J. Mora-Florez, and S. Pérez-Londoño, "Classification methodology and feature selection to assist fault location in power distribution systems," *Revista Facultad de Ingeniería-Universidad de Antioquia* vol. 44, pp. 83–96, June 2008 [Online]. Available: http://ingenieria.udea.edu.co/grupos/revista/revistas/nro044/09rev_44.pdf

[11] J. Mora-Florez, N. Estrada-Cardona, and G. Morales-Espana, "Single phase fault location in power distribution systems using statistical analysis," in *Proc. IEEE/PES Transmission and Distribution Conf. and Expo.: Latin America*, 2008, pp. 1–5.

[12] R. Aggarwal, Y. Aslan, and A. Johns, "New concept in fault location for overhead distribution systems using superimposed components," in *IEEE Proc. Gener., Transmiss., Distrib.*, May 1997, vol. 144, no. 3, pp. 309–316.

[13] D. Novosel, D. Hart, Y. Hu, and J. Myllymaki, "System for Locating Faults and Estimating Fault Resistence in Distribution Networks With Tapped Loads," U.S. Patent 5 839 093, 1998.

[14] M. Saha and E. Rosolowski, "Method and Device of Fault Location for Distribution Networks," U.S. Patent 6 483 435, 2002.

[15] G. Morales-España, H. Vargas-Torres, and J. Mora-Florez, "Impedance based method to fault location in power distribution, considering tapped loads and heavy unbalanced systems," in *Proc. XII Encuentro Regional Iberoamericano del CIGRÉ* , Foz de Iguazú, Brazil, May 2007.

[16] "Load representation for dynamic performance analysis [of power systems]," *IEEE Trans. Power Syst.*, vol. 8, no. 2, pp. 472–482, May 1993.

[17] A. Sepälä, "Load research and estimation in electricity distribution," Ph.D. dissertation, Tech. Res. Center Finland, , 1996.

[18] J. Zhu, D. Lubkeman, and A. Girgis, "Automated fault location and diagnosis on electric power distribution feeders," *IEEE Trans. Power Del.*, vol. 12, no. 2, pp. 801–809, Apr. 1997.

[19] Radial Test Feeders—IEEE Distribution System Analysis Subcommittee [Online]. Available: http://ewh.ieee.org/soc/pes/dsacom/testfeeders.html

[20] J. Dagenhart, "The 40-ground-fault phenomenon," *IEEE Trans. Ind. Appl.*, vol. 36, no. 1, pp. 30–32, Jan./Feb. 2000.

Germán Morales-España received the B.Sc. degree in electrical engineering from the Industrial University of Santander (UIS), Bucaramanga, Colombia, in 2005. He is currently pursuing the M.Sc. degree in engineering and policy analysis at Delft University of Technology (TUDelft), Delft, The Netherlands.

His areas of interest are power quality, protective relaying, economy and regulation of electric sector, and policy analysis.

Mr. Morales-España is a member of GISEL (Col) Research Group on Electric Power Systems.

Juan Mora-Flórez received the B.Sc. degree in electrical engineering from the Industrial University of Santander (UIS), Bucaramanga, Colombia, in 1996, the M.Sc. degree in electrical power from UIS in 2001, the M.Sc. degree in information technologies from the University of Girona (UdG), Girona, Spain, in 2003, and the Ph.D. degree in information technologies and electrical engineering from UdG in 2006.

Currently, he is a Lecturer with the Electrical Engineering School, Technological University of Pereira, Pereira, Colombia. His areas of interest are power quality, transient analysis, protective relaying, and soft computing techniques.

Dr. Mora-Florez is a member of the ICE (Col) Research Group on Power Quality and System Stability.

Hermann Vargas-Torres received the B.Sc. degree in electrical engineering and the M.Sc. degree in electrical power from the Industrial University of Santander (UIS), Bucaramanga, Colombia, in 1985 and 1990, respectively, and the Ph.D. degree in electrical engineering from the Universidad Pontifícia Comillas (UPCO), Madrid, Spain, in 2002.

Currently, he is a Professor with the Electrical Engineering School, UIS. His areas of interest are power systems stability, transient analysis, power quality, protective relaying, and policy analysis.

Dr. Vargas-Torres is a member of the GISEL (Col) Research Group on Electric Power Systems.